A dynamic model for the life history of *Maurolicus muelleri,* a pelagic planktivorous fish

RUNE ROSLAND AND JARL GISKE

Department of Fisheries and Marine Biology, University of Bergen, HIB, N–5020 Bergen, Norway

ABSTRACT

The life history and vertical distribution of a female cohort of the mesopelagic fish *Maurolicus muelleri* is simulated using stochastic dynamic programming. The environment is represented by vertical profiles of zooplankton biomass, light intensity and temperature, all variables changing with season. The fish physiology is modelled by dynamic state variables that represent structural fish weight, energetic state and the age of developing oocytes. The model is used to simulate optimal depth distribution (feeding vs. predation risk) and energy allocation (somatic growth or reproduction). The optimal strategies predicted by the model depend on structural fish weight, energetic state and seasonal factors in the environment. The different strategies predicted for different size groups of fish are consistent with field observations of *M. muelleri*. Small fish give higher priority to growth and tolerate higher levels of predation risk than large fish. The strategies of small fish seem to be little affected by changes in energetic state or seasonal factors in the environment. On the other hand, the predicted strategies of large fish are largely dependent on energetic state and seasonal changes in the environment. In the winter they do not reproduce and minimize visual predation risk by staying at depths with a low light intensity. The low light intensities also result in a low food intake and a negative energy budget in the winter months. In spring, summer and autumn, the predicted strategy of large fish is to stay at depths that provide feeding rates sufficient to rebuild energy reserves lost in the winter and to provide energy for reproduction and somatic growth.

INTRODUCTION

Classical life history theory (LHT) traditionally focused on factors related to survival and fecundity and the trade-off between those factors that maximize reproductive rate (Fisher, 1930; McLaren, 1963; Werner and Gilliam, 1984; Aksnes and Giske, 1990; Leonardson, 1991a,b; Roff, 1992; Stearns, 1992; Vance, 1992; Engen and Sæther, 1994). According to Aksnes and Giske (1990) the trade-off between growth and survival may differ between organisms with constant and variable generation times. By keeping growth rates high, juveniles may potentially benefit from a shorter generation time as well as increased fecundity, while adults may only gain increased weight and fecundity because they are already mature. Aksnes and Giske (1990) showed that increased fecundity alone may not compensate for the increased mortality risk following high growth, thus maximizing survival may be the optimal strategy for organisms with a constant generation time. If, however, high growth leads to a shorter generation time, then the benefits from high growth may compensate for the increased mortality thereby making high growth the optimal strategy for organisms (or life stages) with variable generation times. Giske and Aksnes (1992) suggested that a potential variable generation time could explain the different winter strategies among juveniles and adults of the mesopelagic fish *Maurolicus muelleri*. Size-dependent factors in mortality and growth may also play an important role in optimal habitat selection (Werner, 1988; Werner and Hall, 1988).

LHT calculates the optimal static solution over a given period of time but does not account for fluctuations in the environment or changes in the state of the organism (e.g. size or energy reserves) that may occur within the given time horizon. Such short-time fluctuations may result in strategies that deviate from those predicted by LHT. For organisms living in a seasonal environment with annual reproduction, such as most temperate pelagic fish species, these fluctuations probably occur on time scales shorter than the generation time.

M. muelleri is an example of a fish with annual reproduction that experiences large seasonal fluctuations in the environment. It has a life span of about 3–

4 years in Norwegian fjords, and feeds mainly on co-pepods and euphausiids (Samyshev and Schetinkin, 1971; Gjøsæter, 1981; Young and Blaber, 1986). It seems to mature within one year and produces several batches of eggs during the breeding season lasting from early spring to autumn (Lopez, 1979; Gjøsæter, 1981; Clark, 1982; Young *et al.*, 1987; Melo and Armstrong, 1991; Rasmussen and Giske, 1994; Goodson *et al.*, 1995). It is one of the numerically dominant fish species in western fjords and off the continental shelf of Norway (Gjøsæter, 1981, 1986).

Observations on *M. muelleri* indicate size-dependent and seasonally dependent differences in depth preference, growth and reproduction (Giske *et al.*, 1990; Giske and Aksnes, 1992; Bjelland, 1995; Goodson *et al.*, 1995). The differences between small (juveniles) and large (older and probably adult) fish are most evident in the winter (Giske *et al.*, 1990; Goodson *et al.*, 1995), when large fish prefer deeper locations than small fish and, unlike juveniles, do not migrate to the surface at dawn and dusk. Small fish have high feeding rates while the feeding rates of larger fish are very low in the winter (Giske and Aksnes, 1992). Large fish probably cover their metabolic demands through stored fats (Falk-Petersen *et al.*, 1986) in the winter months. During spring and summer the differences between small and large fish diminish, partly because large fish change priority from survival to growth, and partly because small fish have grown larger and mature some time during early spring and summer (i.e. entering the adult stage). In spring, both age groups migrate to the surface at dawn and dusk, but larger fish seem to be located deeper than small fish during the daytime in early spring and summer (Bjelland, 1995; Goodson *et al.*, 1995). The larger females also seem to allocate surplus energy to the gonads and start producing batches of oocytes earlier than smaller fish (Goodson *et al.*, 1995).

The observed variations in strategies within populations of *M. muelleri* may be explained from individual differences in age, size and energetic state, while some of the variations probably rely on seasonal fluctuations in the environment. Zooplankton, which is the primary food source for *M. muelleri*, generally has a higher biomass in the summer than in the winter (Giske *et al.*, 1991). The availability of zooplankton is also reduced in winter because most of the biomass is located deeper than in the summer (Kaartvedt *et al.*, 1988; Magnesen *et al.*, 1989; Giske *et al.*, 1990; Baliño and Aksnes, 1993; Rasmussen and Giske, 1994; Bjelland, 1995). Zooplankton is therefore relatively less available for visually hunting planktivores, such as *M. muelleri*, in the winter compared with the summer. The

combined effect of different zooplankton biomass and availability at suitable depths may therefore result in large seasonal variations in food availability for planktivores. A high feeding rate (digestion limited) is still possible in shallow water during the winter, as observed for small *M. muelleri*, but the risk of visual predation associated with feeding at this time of the year may be greater than in other seasons (Giske and Aksnes, 1992; Rosland and Giske, 1994).

The observed strategy of large *M. muelleri* in the winter is incompatible with static LHT because negative growth cannot be an optimal lifetime strategy. Negative energy budgets of fish are, however, not uncommon during limited periods such as in winter (Giske and Aksnes, 1992; Paul *et al.*, 1993; Hayes and Rose, 1994; Wang and Houde, 1994). By using stochastic dynamic programming (SDP: Mangel and Clark, 1986, 1988; Houston *et al.*, 1988) the life cycle can be divided into several shorter time units. This makes it possible to account for fluctuations in the environment and the state of the organism that may occur within the life cycle, and to calculate the different trade-offs between growth, survival and reproduction at different times of the life cycle. Through the SDP framework, the many external and internal factors may be compared, and their separate and combined effects on the strategy can be studied.

Over the last 10 years, SDP has been applied to several ecological problems including aquatic systems (Clark and Levy, 1988; Sargent, 1990; Rosland and Giske, 1994; Fiksen and Giske, 1995; Fiksen *et al.*, 1995). With a few exceptions (Fiksen and Giske, 1995; Fiksen *et al.*, 1995), however, SDP has primarily been applied to model distinct phases of the life history and seldom the entire life cycle. Rosland and Giske (1994) developed an SDP model for the diel vertical distribution of two age groups of *M. muelleri*. By giving unequal motivation for growth (Aksnes and Giske, 1990; Giske and Aksnes, 1992), this model exhibited the two sound-scattering layers as observed in the field by Giske *et al.* (1990). Because the model covered only a 24-hour cycle in January, however, it was not ascertained whether or not the assumed difference in the growth motivation that was used as a forcing, was an 'artefact' of the terminal fitness function. Whether size differences in future reproduction or seasonal variation in mortality risk and feeding gain could cause the observed differences in vertical distribution during winter, had to be tested through a life history approach that included all these elements in one model.

The aim of the present work was to develop a dynamic life history model, based on the SDP frame-

work, for a pelagic fish living in a seasonal environment. The model shares many of the same elements as the model by Fiksen *et al.* (1995), with a spatial dimension and state of the organism, but the present model has a finer time resolution and more elaborate state space than that of Fiksen *et al.* (1995).

THE MODEL

Decision variables: depth location and energy allocation

The fish has a finite set of depth locations available each time period, where the depth locations differ in respect to prey encounter rates, temperature and predation risk.

The fish is also in control of the allocation of energy to somatic growth and reproduction (see below). In order to maximize reproductive output, calculated as net reproductive rate in this model, the fish faces the trade-offs between growth and survival and somatic against reproductive energy allocation.

Environment

The model environment represents a seasonal pelagic habitat in a fjord of western Norway and includes surface light, vertical light attenuation and vertical profiles of temperature and zooplankton biomass.

Zooplankton biomass (Fig. 1a) is calculated by a production model for Masfjorden in western Norway (Giske *et al.*, 1991). Model results for zooplankton biomass were preferred to field data because interannual variations in biomass may be large (Giske *et al.*, 1991).

The vertical distribution of zooplankton is based on field data (unpublished) from four different stations in Masfjorden collected with a Juday net at different seasons in the period from 1987 to 1989. The vertical zooplankton biomass distributions in the different months are given as a percentage of the depth-integrated zooplankton biomass (i.e. from the surface to 250 m) in Fig. 1b. These data originate from different years, and we have to assume that the relative vertical distribution of zooplankton is more dependent on season than on year, i.e. zooplankton are generally located close to the surface in the summer and at depth in the winter. The vertical profile of the absolute zooplankton biomass is obtained by distributing the modelled biomass (Fig. 1a) according to the observed vertical distribution (Fig. 1b) in different seasons.

Seasonal vertical temperature profiles are based on field data (unpublished) from Herdlefjorden (in western Norway) and Masfjorden (Fig. 1c).

Surface light was calculated following the same procedures as Rosland and Giske (1994) which were based on a model by Skartveit and Olseth (1988) and data from Rosenberg (1966).

The dynamic state variables

We used three state variables to represent fish physiology: structural weight of the fish, energy content and the age of developing oocytes (Table 1).

The variable for structural fish weight (W) can be considered analogous to fish length, because it represents a standardized fish weight that corresponds to a certain fish length. Structural weight is calculated from length using a length-to-weight regression established by Rasmussen and Giske (1994). Being analogous to fish length, the structural weight (W) is not allowed to decrease in value.

Although energy density may tend to increase with fish weight (Stewart *et al.*, 1982; Hislop *et al.*, 1991; Hewett and Johnson, 1992; Ikeda, 1996), we assumed that energy density (q_f) generally is constant for all weight groups. From the relative body constituents of protein and fat estimated for *M. muelleri* (Anonymous, 1977) it is then possible to calculate the energy density (q_f) of the fish by using energetic coefficients for fat and protein (Elliott, 1976; Mangalik, 1986; Cacho, 1990). The energy density calculated by this approach is by our definition the energy density of fish at a high energetic state. The total amount of energy in fish at a high energetic state at a given structural weight is then found by multiplying the structural fish weight (W) by the energy density of the fish (q_f). The total amount of energy corresponding to the structural fish weight (W) is denoted by the variable $Q(W)$.

To account for negative growth, we included a variable tracking the total amount of energy (E) that changes according to the net energy intake. A negative net energy budget depletes the energy reserves of the fish and will ultimately lead to starvation. During negative growth the variable for fish structural weight (W) remains unchanged. A positive energy budget will eventually increase the structural weight (W), given that the total energy content (E) exceeds the standardized amount of energy $Q(W)$ corresponding to the current weight (W). In other words, a fish with a structural weight W with a total amount of energy (E) below that of the standardized value $Q(W)$, has to rebuild energy reserves, i.e. $E \geq Q(W)$, before further increase in the structural weight can take place.

To account for possible time constraints on reproduction, a variable tracking the age of a developing oocyte (D) was included. The energetic constraints on reproduction are accounted for by the variable for

Figure 1.   (a) Surface-integrated zooplankton biomass (mgC m^{-2}) in different months. (b) Vertical distribution of zooplankton biomass (isolines) as a percentage of total biomass (from 0 to 250 m) in different months. (c) Vertical temperature (°C) profiles (isolines) in different months.
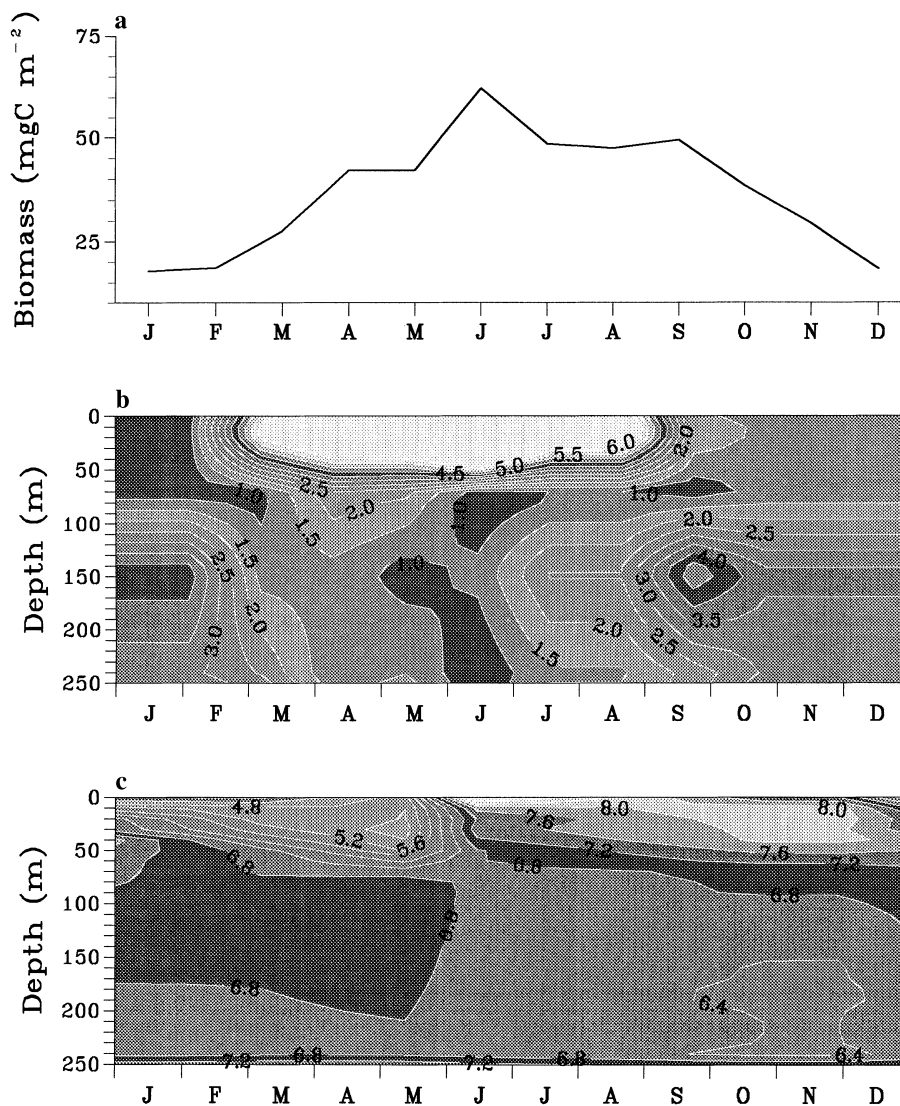
energy content (E). We assume that primary oocytes are a non-depletable resource, and reproduction is modelled as a series of oocyte batches that are developed and spawned one at a time. D tracks the time from onset of the oocyte-ripening process until fully ripe oocytes are produced and spawned. The onset of oocyte production is controlled by the fish (i.e. decision variable), but once the oocyte-ripening process has started, it is irreversible and the fish commits itself to produce and spawn the batch it initiated.

Weight- and length-related variables

Variables such as fecundity, consumption, respiration, predation and vision are all related to the variable for structural weight W, either through regressions (Melo and Armstrong, 1991; Rasmussen and Giske, 1994), or through functional relationships (McGurk, 1986; Hewett and Johnson, 1992; Aksnes and Giske, 1993).

State dynamics

The total energy content (E) is a function of the net growth (G_z) in energy units at depth z in a time interval less the energy lost in oocyte production:

$$E_j = E + G_z - rq_e \ , \tag{1}$$

Table 1. Definition of parameters and variables

Symbol	Description	Unit	Value
$\lambda_{z,j}$	Probability of consumption level j at depth z	–	0–1
τ	Duration of a time interval	day	5
D ‡	Age of developing oocytes	day	0–15
E ‡	Energy content of a fish	joule	–
$F(W,E,D,t,T)$	Fitness function in the SDP (stochastic dynamic programming)	–	–
G_z ‡	Net growth	joule	–
J	Maximum feeding level	–	100%
L_t	Larval survival probability in time t	–	0–1
$Q(W)$	Energy content corresponding to structural weight (W)	joule	–
T	Time horizon of the model	[ ]	292
S_z	Survival probability at depth z	–	0–1
W ‡	Structural fish wet weight	g	0.02–4.00
b	Number of oocytes in a batch	–	[ ]
c *	Energy allocation rule (0 = somatic, 1 = reproduction)	–	0 or 1
j	Feeding level	–	0–100%
q_e	Energy density of a ripe oocyte (Ikeda, 1996)	Jg^{-1}	4700
q_f	Energy density of a fish (Anonymous, 1977)	Jg^{-1}	8685
r	Weight of ripe oocyte batch	g	[ ]
t	Time index	[ ]	[ ]
w	Weight of individual ripe oocyte (Melo and Armstrong, 1991)	g	$1.5 \cdot 10^{-4}$
z *	Depth index	[ ]	1–30
t_D	Oocyte ripening time	day	5

‡These variables occur in the text sometimes with the indices j and c, which indicate that they represent the new states in the end of a time interval.
*The asterisks on these variables indicate the optimal value.

where r denotes the weight of a batch of oocytes, q_e represents the energy density of an oocyte, and the index j indicates the new value of energy content at the end of a time interval (E is the energy content at the beginning of a time interval). The net growth (G_z) depends on prey encounter rate and temperature, and is a function of depth (see sections below on *Prey encounter and feeding rate* and *Growth*).

The dynamics of the variable for structural weight (W) is a function of the energy content (E_j in eqn 1):

$$W_j = \begin{cases} W & \text{if} \quad E_j \leq Q(W) \\ \frac{E_j}{q_f} & \text{if} \quad E_j > Q(W) \end{cases}, \quad (2)$$

where the index j indicates the new value of the weight at the end of a time interval (as in eqn 1). The above equation is a formalized statement saying that if total energy content (E_j) at the end of a time interval is less than or equal to the standardized energy content, $Q(W)$ corresponding to the structural weight (W) at the start of the time interval, then the structural weight remains unchanged. If, however, total

energy content at the end of a time interval is greater than the standardized energy content, $Q(W)$ at the start of a time interval, then the weight is increased to a value (W_j), where the standardized energy content, $Q(W_j)$, equals the actual energy content (E_n) of the fish at the end of the time interval.

The dynamics of the oocyte-ripening process (D) are:

$$D_c = \begin{cases} 0 & \text{if } \{D = 0 \text{ and } c = 0\} \text{ or } \{D = t_D\} \\ D + \tau & \text{if } \{D = 0 \text{ and } c = 1\} \text{ or } \{0 < D < t_D\}, \end{cases} \quad (3)$$

where τ represents the duration of a time interval, and c is the decision variable for onset ($c = 1$) of oocyte production and functions as an index for the new batch state in the end of the time interval. Once a batch of oocytes is in production ($D > 0$) the process is irreversible and continues until the batch is ripe ($D = t_D$) and spawned. The total oocyte mass (r) spawned each time interval therefore depends on the

developmental status of the oocytes (D) and on fecundity which is a function of structural weight (W):

$$r = \begin{cases} 0 & \text{for} \quad D < t_D \\ 0.05W & \text{for} \quad D = t_D \end{cases} . \quad (4)$$

The total number of oocytes spawned (b) equals total oocyte mass (r) divided by the weight of an individual ripe oocyte (w):

$$b = \frac{r}{w} \quad . \quad (5)$$

Observations of M. *muelleri* have indicated different weights at maturity (Gjøsæter, 1981; Rasmussen and Giske, 1994; Bjelland, 1995; Goodson *et al.*, 1995), which might indicate a plasticity of age and weight at maturity (Stearns and Crandall, 1984). We therefore chose not to define a weight threshold for maturity, instead allowing the fish to reproduce at all weights.

The state- (structural fish weight, energy content and oocyte status) and time-dependent fitness ($F[W,E,D,t,T]$), optimal depth position (z^*) and energy allocation (c^*) are calculated in the SDP equations (Mangel and Clark, 1988). Net reproductive rate (R_0) is used here as the fitness currency of the model. State-dependent fitness at time t is calculated as the probability of reaching new states W_j, E_j and D_c, where the state-change probabilities are found from the probabilities of feeding ($\lambda_{z, j}$) and survival (S_z) at depth z at a feeding level j, when using the energy allocation rule c. Additional fitness is gained if a batch of oocytes (b) with an expected larval survival (L_t) is spawned during the time interval t to $t + 1$. The optimal state- and time-dependent depth position (z^*) and allocation rule (c^*) are those that maximize the state-related fitness ($F[W,E,D,t,T]$) at time t:

$$F(W, E, D, t, T) =$$
$$\max_{z,c} \left\{ S_z \sum_{j=0}^{J} \lambda_{z,j} \left[F(W_j, E_j, D_c, t+1, T) + bL_t \right] \right\} .$$
$$(6)$$

The index j represents the feeding level from 0 to J (maximum potential feeding capacity). Equation 6 includes the expected future fitness of the female spawner added to the number of eggs (b) laid in time interval (t) multiplied by survival (L_t) of the larvae in time t. Schultz (1993) found that the survival probability for dwarf perch, *Micrometrus minimus*, was

normally distributed around an optimal birth date, and a similar distribution was applied here to describe larval survival as a function of birth date. Such a seasonal distribution of larval survival does not seem unrealistic given the seasonal distribution of food abundance, daylength and temperature. Maximum larval survival is assumed to occur in mid-June with a variance of 50 days. The variance was tuned to spread reproductive activity to observed dates (Lopez, 1979).

The fitness value at the terminal time interval ($t = T$) is zero, which means that there is no value in surviving to time T only. The fish can therefore only gain fitness by producing eggs between time $t = 1$ and time T.

Prey encounter and feeding rate

Assuming visual foraging only, the prey encounter rate can be expressed as a function of visual range. Visual range depends on light intensity, beam attenuation, visual area and contrast of the prey as well as the sensitivity threshold of the predator's eye (Aksnes and Giske, 1993). Visual range is used to calculate prey detection area (Luecke and O'Brien, 1981; Dunbrack and Dill, 1984). Prey encounter rates are found by multiplying prey detection area by swimming speed (Eggers, 1976) and prey density. Because light intensity declines exponentially with depth, the fish can regulate prey encounter rate through its depth position: depths closer to the surface provide high prey encounter rates while deeper positions provide lower prey encounter rates.

Assuming a stochastic foraging process, the prey encounter events are given a Poisson distribution with expectations equal to the deterministic encounter rate (similar to Rosland and Giske, 1994).

Growth

The net growth (G_z), given in energy equivalents, is calculated using a bioenergetic model (Hewett and Johnson, 1992), where the net growth is a function of food consumption, energy density of the prey, specific dynamic action, egestion, excretion and respiration. The bioenergetic processes are functions of temperature. Besides being limited by the physiological processes, growth may also be limited by prey encounter rates, which are a function of depth position. Depth position also affects the growth rate through temperature which varies between the different depths.

Bioenergetic models have not previously been applied to M. *muelleri* and the parameters therefore had to be based both on field data for M. *muelleri* (Giske *et al.*, 1991; Rasmussen and Giske, 1994; Ikeda, 1996)

and on data for other species including general physiological relationships (Schmidt-Nielsen, 1983; Rudstam, 1989; Hewett and Johnson, 1992).

Time limitations on feeding: stomach effects

The bioenergetic model (Hewett and Johnson, 1992) does not include subprocesses such as stomach evacuation. When daylength (foraging period for visual feeders) is short, the potential consumption may be limited by stomach capacity and evacuation rate. We used an exponential stomach-evacuation model (Jobling, 1981) to account for potential time constraints on the consumption rate. Dividing time-limited stomach evacuation by potential maximum stomach evacuation (at a 24 hour daylength) gives values, ranging from 0 to 1, that can be included in the bioenergetic model to reduce daily consumption ration, according to time constraints on stomach evacuation.

Mortality

The main predators on M. *muelleri* are piscivorous fish (Giske *et al.*, 1990; Rasmussen and Giske, 1994; Bjelland, 1995) such as saithe, *Pollachius virens,* and blue whiting, *Micromesistius poutassou,* that we assume to be visual predators. The vertical distribution of predators may depend on the location of prey, such as M. *muelleri.* A different predator density in the vertical axis could change the vertical predation risk and potentially the optimal depth position of M. *muelleri,* but accounting for this factor would result in a predator–prey interaction that would be difficult to simulate. The optimal strategy of M. *muelleri* is therefore defined under worst-case expectations (i.e. that predators may be present always at all depths), and where the optimal depth is the one that best balances growth and predation risk under the continuous presence of predators. We thus ignore possible vertical differences in predator density. Visual predation risk is calculated from the visual search area of the predator (Giske *et al.*, 1994), which is a function of depth (light intensity and beam attenuation) and size (visibility) of the prey (M. *muelleri*).

The net effect of size dependency in the processes of visual predation risk, prey encounter rate and absolute energetic requirements is that large fish have to pay a relatively higher cost of visual predation risk than small fish in order to maintain their metabolic requirements.

To account for other mortality agents such as non-visual predation, diseases and parasitism, we include a size-dependent mortality factor with an allometric coefficient of 0.25 (McGurk, 1986). Contrary to visual

predation, which is only effective during periods of daylight, the non-visual mortality is always acting on the fish. Contrary to visual predation risk, which may be controlled by the fish through its depth position, non-visual mortality risk is independent of depth position.

The visual mortality coefficient was given the same value as that used by Rosland and Giske (1994), where it was tuned to give the overall mortality around the estimates of adult mortality rates (1.8 per year) found by Gjøsæter (1981).

The inclusion of non-visual mortality here increased the total annual mortality to about 2.5 per year for the model run simulation. The actual values of mortality are difficult to assess and are thus associated with a degree of uncertainty.

Pelagic habitat

The depth positions available to the model fish represent light isolumes with a constant light intensity during daytime which is here defined as the period when surface light intensity is above $0.02\ \mu mol$ $m^{-2}\ s^{-1}$. The actual depth position during daytime will therefore vary with surface light. This definition of depth positions does not account for crepuscular feeding (Rosland and Giske, 1994).

Prey biomass and temperature are calculated for each depth position as the average value from the surface to the depth position at noon. The depth positions defined here will detect the rough seasonal variations in zooplankton vertical distribution and temperature, but will not be able to resolve fine-scale variations in depth variables.

THE SIMULATION

We have simulated the dynamics of a cohort of fish initiated as pre-juveniles (Robertson, 1976) at 0.02 g wet weight (structural weight) and a time horizon (i.e. life expectancy) of 4 years. The time steps are 5 days, but the environmental variables change only monthly. Only the first three model years are presented because terminal effects dominate the model results in the last year of a simulation run.

RESULTS

First year

Lower surface light intensity and reduced prey abundance in winter, combined with a high reward for growth, force the fish to stay at shallower and more illuminated depths (Fig. 2a) to maintain high feeding

Figure 2. Time distribution of: (a) average light intensity (μmol m^{-2} s^{-1}) at the depth of occurrence of each cohort; (b) fraction of initial cohort alive; (c) instantaneous mortality rate (day^{-1}); (d) starvation as a percentage of total mortality. The different lines represent the same cohort in the first (solid), second (dotted) and third (dashed) year.
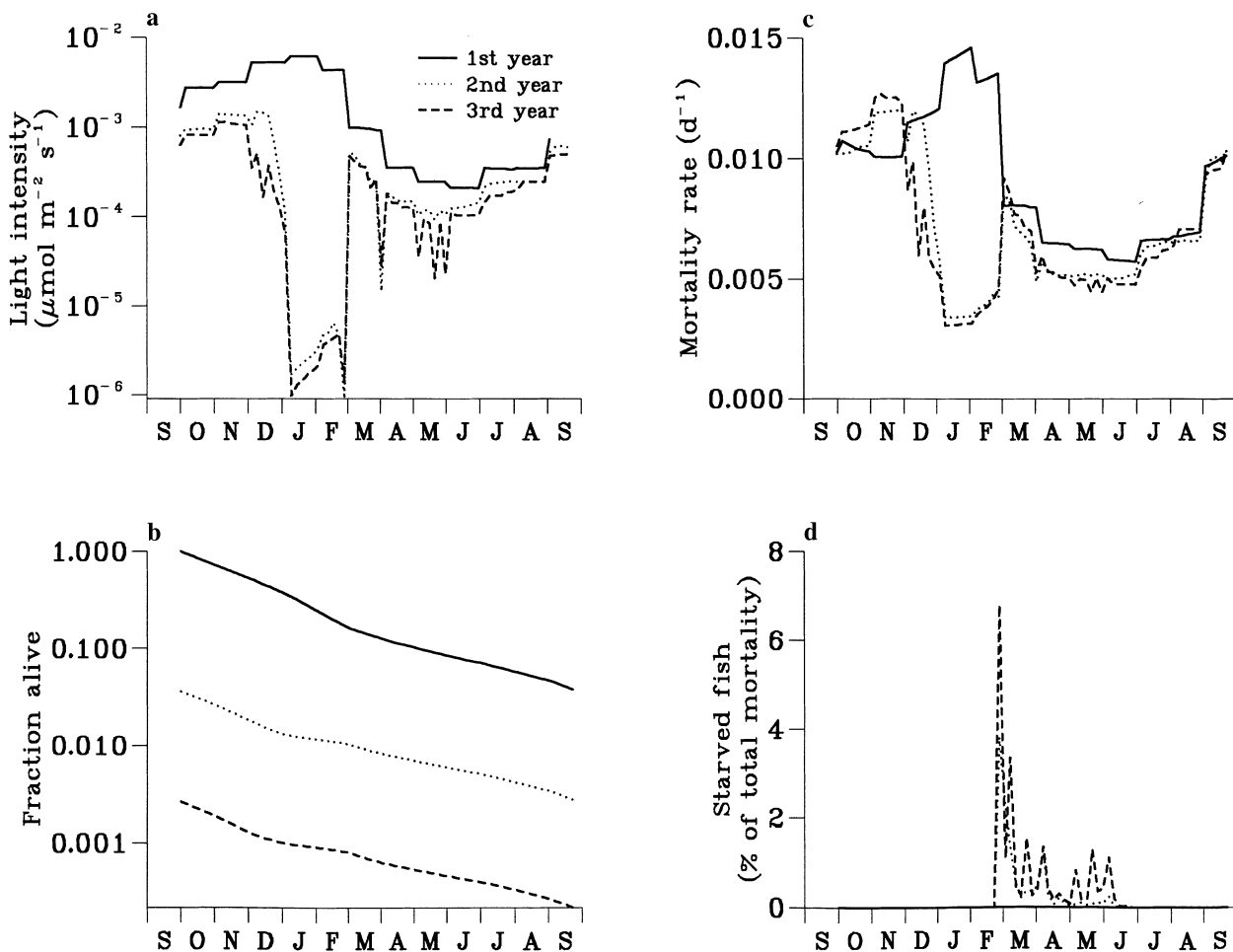

rates in the winter. The relatively higher light intensities at shallow depths in winter result in increased mortality rates (Fig. 2c) because of more intense visual predation. The number of individuals alive in the cohort decreases steadily throughout the first year (Fig. 2b), but as a result of increased predation risk, the rate of decrease is most marked in the winter (Fig. 2b). None of the fish die from starvation during the first year and predation is therefore the only mortality agent (Fig. 2d).

The average daily feeding ration, given as a percentage of the potential maximum consumption capacity in Fig. 3a, is close to maximum during most of the first year, but with a small reduction in the winter. The average growth rate, given as weight-specific energy intake in Fig. 3b, shows an initial maximum and then decreases with fish weight as the fish grow (Fig. 3b). The irregularities in growth (Fig. 3b) are

caused partly by variations in the feeding rate (Fig. 3a) and partly by water temperature (monthly switches).

The fish start allocating energy to gonad development in early March (Fig. 4a), and continue until mid-October, after which energy is directed to somatic growth. No eggs are laid in the non-profitable periods in late autumn and in the winter when larval survival (i.e. the 'reproductive value' of the eggs) is at a minimum (Fig. 4c). The expected fitness of the fish ($F[W,E,D,t,T]$ in eqn 6) is plotted in Fig. 4d, and clearly reflects the distribution of egg values in Fig. 4c. The peak in fitness occurs just before the peak in larval survival because the future reproductive expectations are then at the maximum. As the reproductive season progresses, the value of eggs (i.e. larval survival) in the current season decreases. Future reproduction therefore relies to an increasing extent on the next reproductive season, which is a winter with low

Figure 3. Time distribution of: (a) average individual daily feeding ration as a percentage of maximum potential food consumption capacity; (b) average individual weight-specific growth rate as energy intake per unit body weight (J g^{-1} day^{-1}); (c) average individual fish weight (g wet weight); (d) average individual energy density (kJ g^{-1}). The different lines represent the same cohort in the first (solid), second (dotted) and third (dashed) year.
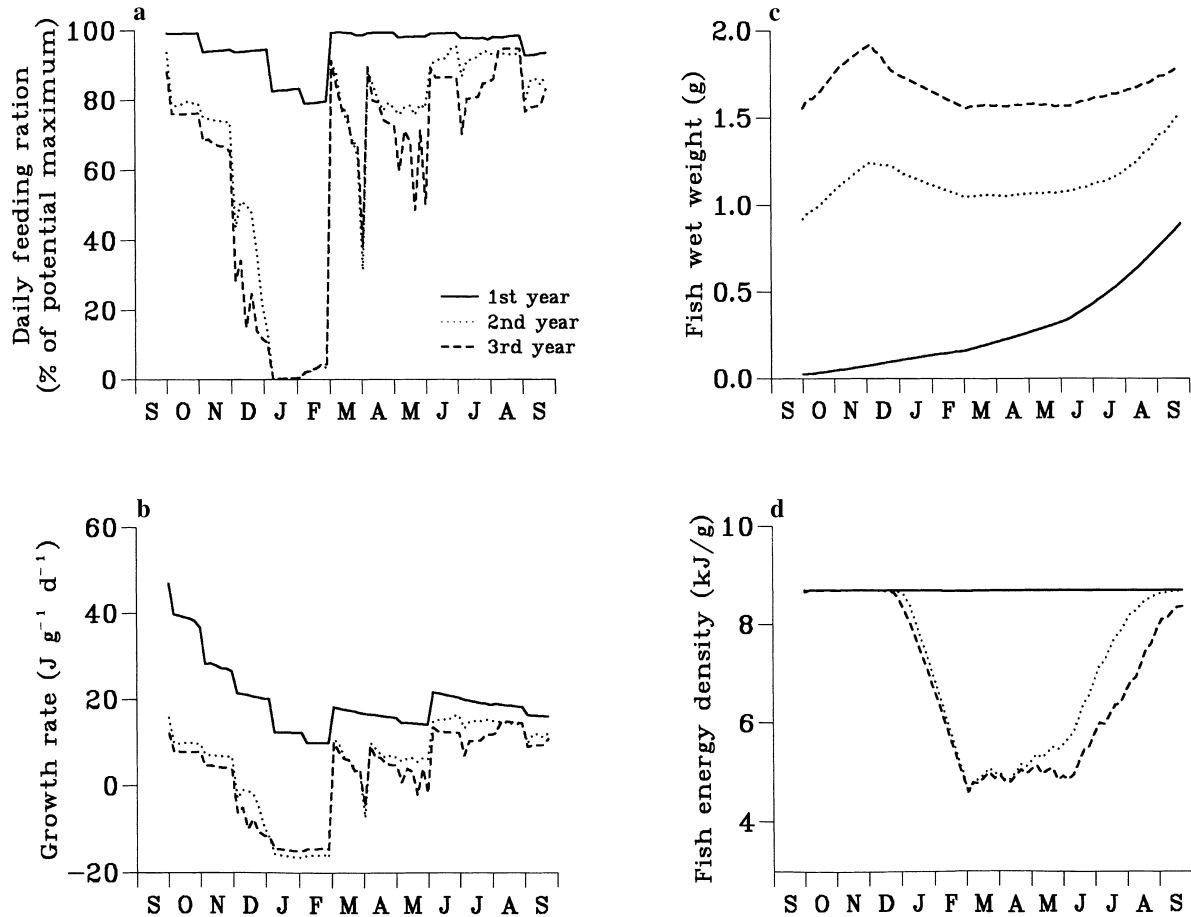
prospects of survival ahead. The expected fitness therefore decreases towards the end of the breeding season.

The average batch fecundity of fish that reproduce (Fig. 4b) shows that the fecundity gradually increases as the breeding season progresses. This is because the fish wet weight increases steadily over the first year (Fig. 3c). The weight plotted in Fig. 3c is, however, not equivalent to W in equations 2–6, but represents the standardized structural weight W minus the calorific difference (recalculated to fat mass) between E, representing current energy content of the fish, and (QW), which represents the standardized energy content corresponding to the structural fish weight W.

Second year

The average wet weight of a fish entering the second year of life is about 0.9 g (Fig. 3c). The feeding rate

starts to decrease from September and reaches a minimum in January (Fig. 3a). The structural fish weight increases towards the end of November, after which feeding rate becomes too low (Fig. 3a) to support metabolic demands (Fig. 3b and d).

The fish prefer deep and less illuminated waters in January and February (Fig. 2a), resulting in low prey encounter rates and a low food intake (Fig. 3a). Because of low food intake the net growth rate becomes negative (Fig. 3b). The fish thus consume energy reserves, which results in decreasing energy density during January and February (Fig. 3d).

Feeding is resumed in March (Fig. 3a) and results in a positive net growth rate (Fig. 3b) which is used to rebuild energy reserves lost during the winter months (Fig. 3d). Energy is allocated to oocyte production from February onwards and continues until mid October (Fig. 4a). The average batch fecundity remains

Figure 4. Time distribution of: (a) the fraction of individuals in the cohort that allocate energy to reproduction; (b) average individual batch fecundity (number of oocytes) of fish reproducing; (c) the value of eggs spawned (i.e. the survival of the resulting larvae); (d) average individual expected fitness. The different lines represent the same cohort in the first (solid), second (dotted) and third (dashed) year.
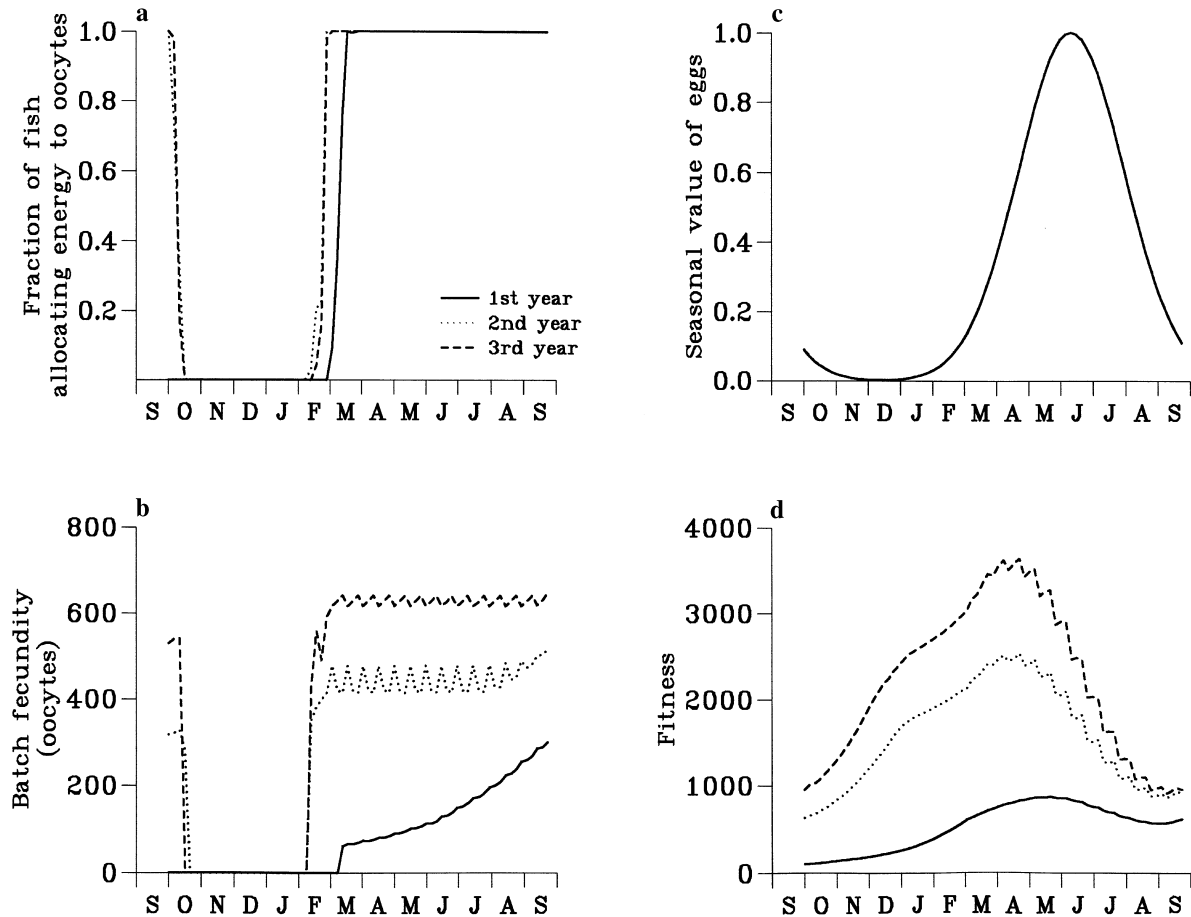
fairly constant over the breeding season (Fig. 4a) because the fish structural weight is then fairly constant (Fig. 3c).

Seasonal trends in the mortality rate (Fig. 2c) only partly correlate with those of the feeding rate (Fig. 3a) because the seasonal variations in prey abundance (zooplankton in Fig. 1a and 1b) change the predation risk that follows from feeding. Although the feeding (Fig. 3a) and growth rates (Fig. 3b) are at a maximum in the summer, the mortality rate (Fig. 2c) is less here than in spring and autumn. This is because of the high prey abundance in the summer (Fig. 1) which makes feeding less costly, measured in terms of visual predation risk, compared with the other seasons.

During the reproductive season a small fraction of fish die from starvation (Fig. 2d). The maximum occurs in the early spring, when as much as 4% of the total mortality is caused by starvation.

Third year

At the start of the third year, the average structural fish weight is about 1.6 g wet weight, and it increases to about 1.9 g in December (Fig. 3c). Most of the patterns in the third year are similar to those in the second year (Figs 2–4), although wet weight (Fig. 3c) and fecundity (Fig. 4b) are higher. In the third year, starvation accounts for a higher fraction of total mortality (up to 7% in early spring – Fig. 2d). This is partly because these fish stay at depths with lower intensity (Fig. 2a), resulting in reduced food intake (Fig. 3a) and increased risk of starvation, but also experience reduced risk of visual predation. Because of their larger size, these fish are also less vulnerable to tactile predation.

Seasonal and physiological effects

The optimal depth positions for four weight categories of fish at two energetic states (high and low) were tracked throughout the year to test the influence of season, weight and energetic state on optimal depth. Optimal depth position (Fig. 5a and 5b), weight-specific prey encounter rate (Fig. 5c and d) and probability of surviving a time interval of 5 days (Fig. 5e and 5f) are given for fish at low and high energetic states at four different weight categories (0.1, 0.5, 1.0 and 2.0 g wet weight).

There is a gradual difference between weight categories of the fish, with the differences being most pronounced in the winter months. Large fish at a high energetic state generally prefer deeper locations

(Fig. 5a and 5b) with lower prey encounter rates (Fig. 5c and 5d) and higher survival (Fig. 5e and 5f) than smaller fish and fish at a low energetic state. The optimal balance between growth and survival for large fish depends on the energetic state, and they switch towards growth-directed behaviour when the energetic state is low. Optimal depth, survival and encounter rates of small (0.1 g wet weight) fish seem less affected by energetic state, i.e. they always tend to stay at depths where the potential growth rate is high.

Using other optimization criteria

The predictions from the SDP model were compared with two other optimization criteria: to maximize the ratio between feeding and mortality 'max. (f/M)'

Figure 5. Seasonal variations in optimal depth position (a and b), prey encounter rate (c and d) and survival (e and f) at different weights and energetic states (low in the figures on the left: a, c and e, and high in the figures on the right: b, d and f). The different lines represent different weights: 0.1 g (solid lines), 0.5 g (dotted lines), 1.0 g (short dashed lines) and 2.0 g (long dashed lines).
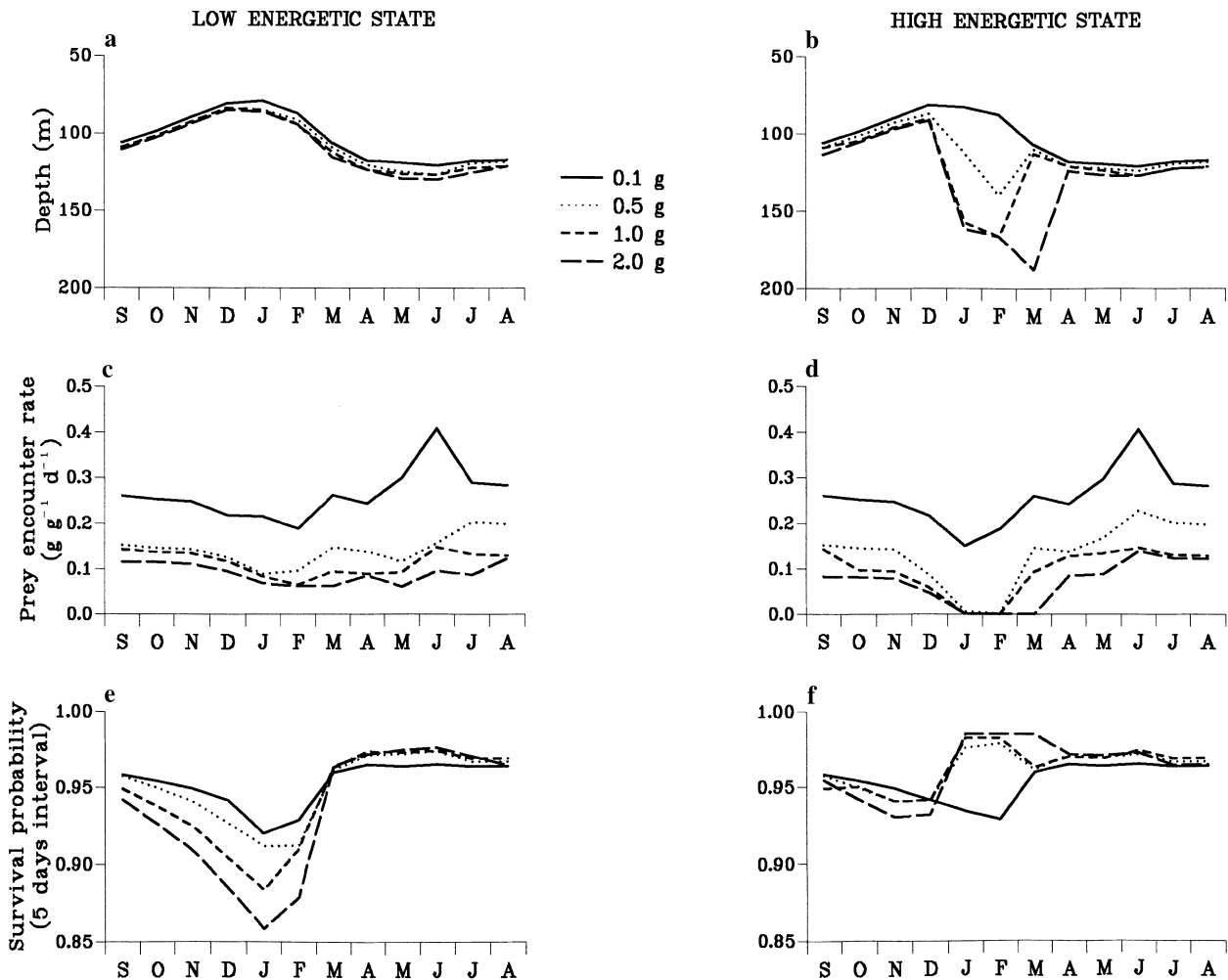
(Werner and Gilliam, 1984) and to maximize growth 'max. (G)' as in traditional optimal foraging theory (Charnov, 1976). The predictions of vertical fitness profiles (VFPs) using the different optimization criteria were carried out for two size groups of fish (0.1 and 1.0 g wet weight) in January and July. VFPs were predicted for fish at both high and low energetic states in the SDP model.

The VFPs predicted by SDP in January for small fish (0.1 g wet weight) at a high and a low energetic condition have similar maxima (Fig. 6a). The VFP for fish at a low energetic state, however, shows a stronger reduction with depth than for fish at a high energetic state. This is because the risk of starvation is higher for fish at a low energetic state. The optimal depth predicted by the SDP is located slightly above that of the 'max. (f/M) rule' but below the 'max. (G) rule' (Fig. 6a).

The VFPs for fish at 0.1 g wet weight in July resemble the profiles in January (Fig. 6c) although some small differences are evident. The optimal depth position predicted by SDP is now located at the same position as predicted by the 'max. (f/M) rule', but still below the 'max. (G) rule'. The similarities between VFPs from January and July indicate that the strategy for small fish is relatively independent of the season.

The VFPs predicted by SDP for large fish at a high energetic state in January (Fig. 6b) resemble a vertical profile of survival from visual predation. The optimal depth is deep (i.e. maximum survival) although the fitness differences are small below a depth of 110 m. Fish at a low energetic state have their fitness max-

Figure 6.   The vertical fitness profiles for two size groups of fish (0.1 and 1.0 g wet weight) derived from stochastic dynamic programming (SDP) for fish at low (SDP(L): solid lines) and high (SDP(H): dotted lines) energetic states and from simpler static rules such as 'maximize feeding over mortality' (f/M: short dashed lines) and 'maximize growth' (G: long dashed lines). The figures represent: (a) 0.1 g fish in January; (b) 1.0 g fish in January; (c) 0.1 g fish in July; and (d) 1.0 g fish in July. To get the fitness profiles from the different rules in the same range of values, each fitness profile was divided by its own maximum to fit in the range (0–1).
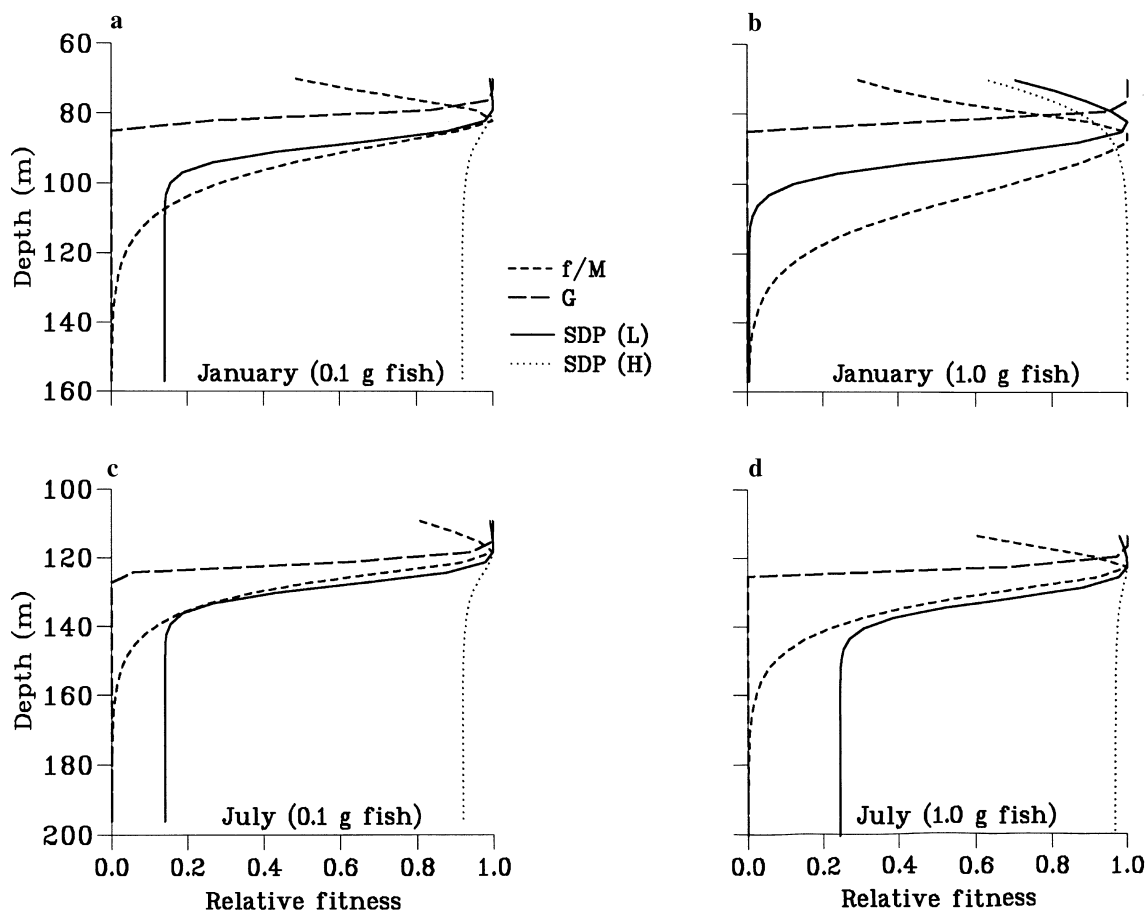
imum located around 85 m, just above the 'max. (f/M) rule', and the VFP resembles those of the small fish (Fig. 6a). Differing from the VFPs for small fish, however, the VFP predicted by SDP for large fish at low energetic state shows a strong decline in fitness above the optimal depth.

The VFPs for large fish in July resemble those of small fish, and the optimal depth position predicted by SDP is located at the same depth as predicted by the 'max. (f/M) rule'.

DISCUSSION

In the following we will refer to each year as the period from September to September. To avoid a repeated specification of which age groups are discussed we will denote 1 group fish as those in the first year and 2+ group fish as those in the second and third years.

Model results and field observations

The model predicts a clear difference in optimal depth position (Fig. 2a), mortality (Fig. 2c), feeding (Fig. 3a) and growth (Fig. 3b) between 1 group and 2+ group fish during the winter. This is consistent with field observations of *M. muelleri* in Masfjorden (Giske *et al.*, 1990; Giske and Aksnes, 1992; Baliño and Aksnes, 1993) and Herdlefjorden (Goodson *et al.*, 1995).

The 2+ group fish in the model change the trade-off between growth and mortality when the breeding season approaches. They enter depth positions with higher light intensities (Fig. 2a), improved feeding conditions (Fig. 3a) and higher growth rates (Fig. 3b) relative to the winter. This prediction is also consistent with field observations from Masfjorden and Herdlefjorden in March (Bjelland, 1995) and Masfjorden in June (Rasmussen and Giske, 1994), indicating that all age and size groups have relatively high feeding rates in spring and summer. Larger fish were, however, located deeper during the daytime, which indicates an intensified crepuscular feeding mode (Rasmussen and Giske, 1994; Rosland and Giske, 1994; Bjelland, 1995). Dividing the time horizon into time units that could account for crepuscular feeding (as in the diel model by Rosland and Giske, 1994) was not possible due to dimensional problems. Feeding was therefore calculated as if the feeding rate was distributed evenly over the period with daylight. This simplification may lead to an erroneous relationship between predation risk and growth that potentially increases if there is a non-linearity between predation risk and feeding rate at different light regimes.

The 2+ group fish in the model start allocating energy to oocytes in February (Fig. 4a) while 1 group fish do not start reproductive energy allocation until March (Fig. 4a). Goodson *et al.* (1995) also found that small immature fish allocated energy to somatic growth during the spring and did not start reproducing until late spring and summer, while larger fish started reproducing earlier. Rasmussen and Giske (1994) found that reproductive allocation was positively correlated with fish size for the smallest fish, while it was constant for larger fish. This latter mechanism is not included here because fecundity is defined as being constant for all size groups once the decision to produce eggs is taken. The energy-allocation rule of the current model is therefore a 'switch decision' (reproduce or not) with no intermediate levels of energy allocation.

Ecological considerations

The sensitivity to changes in energetic condition and seasonal fluctuations in the environment depends on fish weight (Figs 5 and 6). The vertical fitness profiles (VFPs) in Fig. 6 indicate an underlying difference in the depth profitability between large and small fish in the winter. Energetic condition has little effect on the optimal depth for small fish (Fig. 6a), although the vertical fitness gradients are much stronger for fish at a low energetic state below the optimal depth.

The predicted VFP by SDP for well-conditioned large fish in the winter (Fig. 6b) resembles a vertical gradient of survival from visual predation and indicates that survival is the dominating factor in the strategies of large fish in the winter. When visual predation dominates the mortality risk it is therefore optimal to stay deep. At low energetic states, the risk of starvation increases and the fish have to move towards depths with higher light intensities and an increased probability of prey encounter (Fig. 6b). The VFP for large fish at a low energetic state resembles that of small fish (Fig. 6a) except that it decreases strongly above the optimal depth (Fig. 6b). This indicates that the growth motivation is caused by the increased risk of starvation at a low energetic state, and that rapid growth is countered by increased visual predation risk for large fish in the winter. The VFP for small fish, however, declines only slightly above the optimal depth (Fig. 6a). This indicates that the fitness reward from rapid growth is high, and almost compensates the risk from visual predation even above the optimal depth position (i.e. small fish get a large payoff by increasing their structural weight).

In July the optimal depths predicted by SDP (Fig. 6c and 6d) equal those of the 'max. (f/M) rule' for

both size groups. The VFP predicted by SDP also resembles the vertical gradients from the 'max. (f/M) rule', but is missing the strong decline in fitness values above the optimal depth position. In the summer the rewards from growth are high for large fish also, partly because of energy requirements for reproduction and partly because they have to rebuild energy reserves lost in the winter (Fig. 3d). By following the 'max. (f/M) rule' they will maximize the number of offspring produced per unit mortality.

To generalize: small fish follow a strategy that gives higher priority to growth than predicted by the 'max. (f/M) rule' in the winter, but they adapt the 'max. (f/M) rule' in the summer. As a result of reduced prey availability in the winter, the visual predation risk at a given level of feeding intensity is higher in the winter compared with other seasons. For large fish, the increased fecundity that would be gained from high growth in the winter is countered by the strong reduction in survival, and the strategy is therefore to minimize mortality from predators. When the breeding season approaches, they start feeding to rebuild energy reserves and to reproduce. The optimal strategy is then to follow the 'max. (f/M) rule', i.e. maximize offspring production at the minimum expense of predation.

Because this model does not include a weight threshold for maturity, there is no forcing on small fish to grow fast in order to shorten the generation time (Aksnes and Giske, 1990; Giske and Aksnes, 1992). The size-dependent differences in depth preference, growth and mortality predicted here thus result from size dependencies in the processes of prey encounter, growth and mortality. As mentioned above, we did not include a maturation threshold in age or weight because of the potential plasticity in these variables (Stearns and Crandall, 1984). However, to assume that the fish can mature at all sizes and ages is probably not correct either. Given that slow growth may cause delayed maturity, the benefits from reduced generation times (Aksnes and Giske, 1990; Giske and Aksnes, 1992) may well act as a forcing on juveniles to keep growth rates high. Such an additional forcing on growth could potentially increase the predicted difference in depth preference, growth and mortality between juvenile and adult fish.

The optimal strategies predicted here do not account for potential density effects in competition and predation. Observations on populations of M. *muelleri* do indicate temporal density variations in the sound-scattering layers (Giske *et al.*, 1990; Baliño and Aksnes, 1993; Bjelland, 1995; Goodson *et al.*, 1995) and indicate that density-dependent processes may influence their depth distribution.

Model evaluation

There is inevitably a degree of uncertainty connected with both environmental variables and the physiology of M. *muelleri*. We have therefore concentrated on the qualitative aspects rather than emphasizing the quantitative aspects of the model predictions. Within these constraints, the model appears to follow the trends in the life history of M. *muelleri* such as the seasonal and size differences in depth preference, feeding, growth and reproductive patterns. Some of the predictions are not easily verified, such as the predictions of depth preference and energetic state and mortality rates.

It is, however, promising if the qualitative predictions fit the observations because it demonstrates the potential to model fish populations with models that aim to describe the fundamental processes of the system. Including the biological forces that act in the system is an important step to improve the quality and realism of models that intend to represent biological systems. If the underlying model concept is working, then the quantitative predictions may be enhanced by improving the submodels for processes (e.g. improved submodels for growth, prey encounter, inclusion of density dependence) and by improving the input data to the model (such as prey distribution and abundance, mortality risk and seasonal larval survival).

Future work

The model presented here resembles the approach suggested by Giske *et al.* (1992), and includes many of the elements outlined by Tyler and Rose (1994) as crucial to fish population models: heterogeneous individuals in a heterogeneous environment acting to maximize fitness with a mechanistic description of the processes involved in growth and survival. The use of SDP is one way to approach an individual-based model with fitness-based forcing functions; the use of static optimization rules as suggested by Fiksen *et al.* (1995) is an alternative. As demonstrated here, the optimal strategy (rule) may change with physiological condition and time (weight and season), and models based on fixed rules face the problem that the rules may prove incorrect for some situations. In contrast to most other techniques, SDP includes current state (physiology or other crucial variables), environment and future expectations into the calculation of optimal strategy. This makes it possible to imitate the evolutionary 'knowledge' that has accumulated into the genetics of animals through their evolutionary history. On the other hand, SDP is computationally heavy and there are ecological factors such as density dependence and predator–prey interactions that are hard to simu-

late by SDP. The problem with density dependence in competition and predation is possibly better solved by 'rule-based models' such as the use of modified ideal free distribution models expressing predation and feeding as density-dependent variables (Hugie and Dill, 1994; Giske *et al.*, in press).

REFERENCES

Aksnes, D.L. and Giske, J. (1990) Habitat profitability in pelagic environment. *Mar. Ecol. Prog. Ser.* **64**:209–215.

Aksnes, D.L. and Giske, J. (1993) A theoretical model of aquatic visual feeding. *Ecol. Mod.* **67**:233–250.

Anonymous (1977) Laksesild. *Fiskets Gang* **77** (2): 51–52.

Baliño, B.M. and Aksnes, D.L. (1993) Winter distribution and migration of the sound scattering layers, zooplankton and micronekton in the Masfjord, western Norway. *Mar. Ecol. Prog. Ser.* **102**:35–50.

Bjelland, O. (1995) *Life-history tactics of two fjord populations of Maurolicus muelleri.* Cand. scient. thesis, Univ. Bergen, Department of Fisheries and Marine Biology. 42 pp.

Cacho, O. (1990) Protein and fat dynamics in fish: a bioenergetic model applied to aquaculture. *Ecol. Mod.* **50**:33–56.

Charnov, E.L. (1976) Optimal foraging: the marginal value theorem. *Theor. Popul. Biol.* **9**:129–136.

Clark, C.W. and Levy, D.A. (1988) Diel vertical distribution by juvenile sockeye salmon and the antipredation window. *Am. Nat.* **131**:271–288.

Clark, T.A. (1982) Distribution, growth and reproduction of the lightfish *Maurolicus muelleri* (Sternoptychidae) off South-East Australia. *CSIRO Mar. Lab. Rep.* No. 145. 10 pp.

Dunbrack, R.L. and Dill, L.M. (1984) Three-dimensional prey reaction field of the juvenile Coho salmon (*Oncorhynchus kisutch*). *Can. J. Fish. Aquat. Sci.* **41**:1176–1182.

Eggers, D.M. (1976) Theoretical effects of schooling by planktivorous fish predators on rate of prey consumption. *J. Fish. Res. Bd Can.* **33**:1964–1971.

Elliott, J.M. (1976) Body composition of brown trout (*Salmo trutta* L.) in relation to temperature and ration size. *J. Anim. Ecol.* **45**:273–289.

Engen, S. and Sæther, B. (1994) Optimal allocation of resources to growth and reproduction. *Theor. Popul. Biol.* **46**:232–248.

Falk-Petersen, I., Falk-Petersen, S. and Sargent, J.R. (1986) Nature, origin and possible roles of lipid deposits in *Maurolicus muelleri* (Gmelin) and *Benthosema glaciale* (Reinhart) from Ullsfjorden, Northern Norway. *Polar Biol.* **5**:235–240.

Fiksen, Ø. and Giske, J. (1995) A dynamic optimization model for vertical distribution of copepods. *ICES J. Mar. Sci.* **52**:483–503.

Fiksen, Ø., Giske, J. and Slagstad, D. (1995) A spatially explicit fitness-based model of capelin migrations in the Barents Sea. *Fish. Oceanogr.* **4**:193–208.

Fisher, R.A. (1930) *The Genetical Theory of Natural Selection.* Oxford: Clarendon Press, 291 pp.

Giske, J. and Aksnes, D.L. (1992) Ontogeny, season and trade-offs: vertical distribution of the mesopelagic fish *Maurolicus muelleri*. *Sarsia* **77**:253–261.

Giske, J., Aksnes, D.L., Baliño, B.M., Kaartvedt, S., Lie, U., Nordeide, J.T., Salvanes, A.G.V., Wakili, S.M. and Aadnesen, A. (1990) Vertical distribution and trophic interactions of zooplankton and fish in Masfjorden, Norway. *Sarsia* **75**:65–81.

Giske, J., Aksnes, D.L. and Fiksen, Ø. (1994) Visual predators, environmental variables and zooplankton mortality risk. *Vie Milieu* **44**:1–9.

Giske, J., Aksnes, D.L., Lie, U. and Wakili, S.M. (1991) Computer simulation of pelagic production in Masfjorden, Western Norway, and its consequences for production of released 0-group cod. *ICES Mar. Sci. Symp.* **192**:161–175.

Giske, J., Skjoldal, H.R. and Aksnes, D.L. (1992) A conceptual model of distribution of capelin in the Barents Sea. *Sarsia* **77**:147–156.

Giske, J., Rosland, R., Berntsen, J. and Fiksen, Ø. (in press) Ideal free distribution of copepods under predation risk. *Ecol. Mod.* **95**:45–59.

Gjøsæter, J. (1981) Life history and ecology of *Maurolicus muelleri* (Gonostomatidae) in Norwegian waters. *FiskDir. Skr. Ser. Havus.* **17**:109–131.

Gjøsæter, J. (1986) Estimates of the abundance of mesopelagic fish off southern Norway and west of the British Isles 1971–1976. *Flødevigen Rapp.* 1986 **1**: 1–22.

Goodson, M., Giske, J. and Rosland, R. (1995) Growth and ovarian development of *Maurolicus muelleri* during spring. *Mar. Biol.* **124**:185–195.

Hayes, D.B. and Taylor, W.W. (1994) Changes in the composition of somatic and gonadal tissues of yellow perch following white sucker removal. *Trans. Am. Fish. Soc.* **123**:204–216.

Hewett, S.W. and Johnson, B.J. (1992) *An upgrade of a generalized bioenergetics model of fish growth for microcomputers.* Madison, WI: University of Wisconsin, Wisconsin Sea Grant College Program, Sea Grant Technical Report, WIS-SG-92250, 79 pp.

Hislop, J.R.G., Harris, M.P. and Smith, J.G.M. (1991) Variation in the calorific value and total energy content of lesser sandeel (*Ammodytes marinus*) and other fish preyed on by seabirds. *J. Zool. (London)* **224**:501–517.

Houston, A., Clark, C., McNamara, J.M. and Mangel, M. (1988) Dynamic models in behavioural and evolutionary ecology. *Nature (London)* **332**:29–34.

Hugie, D.M. and Dill, L.M. (1994) Fish and game: a game theoretic approach to habitat selection by predators and prey. *J. Fish Biol.* **45** (Suppl. A):151–169.

Ikeda, T. (1996) Metabolism, body composition, and energy budget of the mesopelagic fish *Maurolicus muelleri* in the Sea of Japan. *Fishery Bull.* **94**:49–58.

Jobling, M. (1981) Mathematical models of gastric emptying and the estimation of daily rates of food consumption for fish. *J. Fish Biol.* **19**:245–257.

Kaartvedt, S., Aksnes, D.L. and Aadnesen, A. (1988) Winter distribution of macroplankton and micronekton in Masfjorden, western Norway. *Mar. Ecol. Prog. Ser.* **45**:45–55.

Leonardson, K. (1991a) Predicting risk-taking behaviour from life-history theory using static optimization technique. *Oikos* **60**:149–154.

Leonardson, K. (1991b) Spatial size variation in adult females of *Saduria entomon* (Crustacea, Isopoda): a comparison between field observations and predictions of a life-history model. *Ophelia* **34**:91–104.

Lopez, P.D.C. (1979) Eggs and larvae of *Maurolicus muelleri* (Gonostomatidae) and other fish eggs and larvae from two fjords in western Norway. *Sarsia* **64**:199–210.

Luecke, C. and O'Brien, W.J. (1981) Prey location volume of a planktivorous fish: a new measure of prey vulnerability. *Can. J. Fish. Aquat. Sci.* **38**:1264–1270.

McGurk, M.D. (1986) Natural mortality of marine fish eggs and larvae: role of spatial patchiness. *Mar. Ecol. Prog. Ser.* **34**:227–242.

McLaren, I. (1963) Effects of temperature on growth of zooplankton, and the adaptive value of vertical migration. *J. Fish. Res. Bd Can.* **20**:685–727.

Magnesen, T., Aksnes, D.L. and Skjoldal, H.R. (1989) Finescale vertical structure of a summer zooplankton community in Lindaspollene, western Norway. *Sarsia* **74**:115–126.

Mangalik, A. (1986) *Dietary energy requirements of channel catfish.* PhD diss., Auburn Univ., Auburn, AL. 138 pp.

Mangel, M. and Clark, C.W. (1986) Towards a unified foraging theory. *Ecology* **67**:1127–1138.

Mangel, M. and Clark, C.W. (1988) *Dynamic Modeling in Behavioral Ecology.* Princeton, NJ: Princeton University Press, 308 pp.

Melo, Y.C. and Armstrong, M.J. (1991) Batch spawning behaviour in lightfish *Maurolicus muelleri.* *S. Afr. J. Mar. Sci.* **10**:125–130.

Paul, A.J., Paul, J.M. and Smith, R.L. (1993) The seasonal changes in somatic energy content of Gulf of Alaska yellowfin sole, *Pleuronectes asper.* *J. Fish Biol.* **43**:131–138.

Rasmussen, O.I. and Giske, J. (1994) Life-history parameters and vertical distribution of *Maurolicus muelleri* in Masfjorden in summer. *Mar. Biol.* **120**:649–664.

Robertson, D.A. (1976) Planktonic stages of *Maurolicus muelleri* (Teleostei: Sternoptychidae) in New Zealand waters. *N. Z. J. Mar. Freshwater Res.* **10**:311–328.

Roff, D.A. (1992) *The Evolution of Life Histories.* New York: Chapman & Hall, 535 pp.

Rosenberg, G.V. (1966) *Twilight – A Study of Atmospheric Optics.* New York: Plenum Press, 358 pp.

Rosland, R. and Giske, J. (1994) A dynamic optimization model for the diel vertical distribution of a pelagic planktivorous fish. *Prog. Oceanog.* **34**:1–43.

Rudstam, L.G. (1989) Exploiting the dynamics of herring consumption in the Baltic: applications of an energetics model of fish growth. *Kieler Meerforsch., Sonderh.* **6**:312–322.

Samyshev, E.Z. and Schetinkin, S.V. (1971) Feeding patterns of some species of Myctophidae and *Maurolicus muelleri* caught in the sound dispersing layers in the north-western African area. *Ann. Biol. CIEM* **28**:212–215.

Sargent, R.C. (1990) Behavioural and evolutionary ecology of fishes: conflicting demands during the breeding season. *Ann. Zool. Fenn.* **27**:101–118.

Schmidt-Nielsen, K. (1983) *Animal Physiology: Adaptation and Environment,* 3rd edn. Cambridge: Cambridge University Press, 619 pp.

Schultz, E.T. (1993) The effect of birth date on fitness of female dwarf pearch, *Micrometrus minimus.* *Evolution* **47**:520–539.

Skartveit, A. and Olseth, J.A. (1988) *Varighetstabeller for timevis belysning mot 5 flater pa 16 norske stasjoner.* University of Bergen, Meteorological Report Series 7, 136 pp.

Stearns, S.C. (1992) *The Evolution of Life Histories.* Oxford: Oxford University Press, 249 pp.

Stearns, S.C. and Crandall, R.E. (1984) Plasticity for age and size at sexual maturity: a life-history response to unavoidable stress. In: *Fish Reproduction, Strategies and Tactics.* G. W. Potts and R. J. Wootton (eds). London: Academic Press, pp. 410.

Stewart, D., Weininger, D., Rottiers, D.V. and Edsall, T.A. (1982) An energetic model for lake trout, *Salvelinus namaycush:* application to the Lake Michigan population. *Can. J. Fish. Aquat. Sci.* **40**:681–698.

Tyler, J.A. and Rose, K.A. (1994) Individual variability and spatial heterogenity in fish population models. *Rev. Fish Biol. Fish.* **4**:91–123.

Vance, R.R. (1992) Optimal somatic growth and reproduction in a limited, constant environment: organisms with determinate growth. *J. Theor. Biol.* **157**:31–50.

Wang, S.B. and Houde, E.D. (1994) Energy storage and dynamics in bay anchovy *Anchoa mitchilli.* Mar. Biol. **121**:219–227.

Werner, E.E. (1988) Size, scaling, and the evolution of complex life cycles. In: *Size-structured Populations: Ecology and Evolution.* B.Ebenham and L. Persson (eds). Berlin: Springer Verlag, pp. 284.

Werner, E.E. and Gilliam, J.F. (1984) The ontogenetic niche and species interactions in size-structured populations. *Ann. Rev. Ecol. Syst.* **15**:393–425.

Werner, E.E. and Hall, D.J. (1988) Ontogenetic habitat shift in bluegill: the foraging rate-predation risk trade-off. *Ecology* **69**:1352–1356.

Young, J.W. and Blaber, S.J.M. (1986) Feeding ecology of three species of midwater fishes associated with the continental slope of eastern Tasmania, Australia. *Mar. Biol.* **93**:147–156.

Young, J.W., Blaber, S.J.M. and Rose, R. (1987) Reproductive biology of three species of midwater fishes associated with the continental slope of eastern Tasmania, Australia. *Mar. Biol.* **95**:323–332.